

CNWRA *A center of excellence in earth sciences and engineering*

A Division of Southwest Research Institute®
6220 Culebra Road • San Antonio, Texas, U.S.A. 78228-5166
(210) 522-5160 • Fax (210) 522-5155

April 22, 2003
Contract No. NRC-02-02-012
Account No. 06002.01.051

U.S. Nuclear Regulatory Commission
ATTN: Dr. John S. Trapp
Office of Nuclear Material Safety and Safeguards
Two White Flint North, Mail Stop 7 D13
Washington, DC 20555

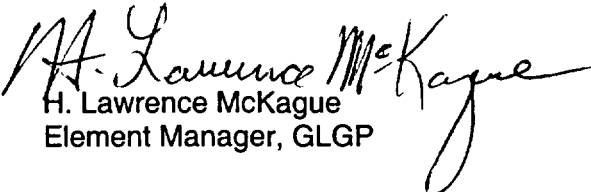
Subject: Completion of Intermediate Milestone— Magma-Tectonic Interactions in Nicaragua: The 1999 Seismic Swarm and Eruption of Cerro Negro Volcano (IM 06002.01.051.375)

Dear Dr. Trapp:

Attached is IM 06002.01.051.375, entitled "Magma-Tectonic Interactions in Nicaragua: The 1999 Seismic Swarm and Eruption of Cerro Negro Volcano." This report documents work conducted as part of the Igneous Activity Key Technical Issue. Field data collected during the 1999 eruption of Cerro Negro volcano are used to develop a model for tectonically induced eruption of basaltic magma. For this eruption, changes in crustal stress produced by tectonic strain reduce the amount of pressure necessary for a partially degassed magma to rise and erupt at Cerro Negro. Tectonically induced fractures can dilate in response to magmatic pressures that are lower than required to propagate and dilate new fractures in the absence of tectonic strain. Observed 1999 eruption rates can be explained by a simplified flow model, which supports the interpretation of low magmatic pressures.

This work demonstrates that small-volume basaltic magmas can ascend from crustal depths without having internal fluid pressures in excess of hydrofracturing pressure, and that magmatic pressures in some eruptions may be only slightly above lithostatic confining pressure. These results help constrain the range of parameters used to evaluate subsurface magma ascent and flow processes for potential magma-repository interactions. If you have any questions, please contact Dr. Brittain Hill at (210) 522-6087 or me at (210) 522-5183.

Sincerely,


H. Lawrence McKague
Element Manager, GLGP

HLM:rae
Attachment

cc:	M. Leach	E. Whitt	K. Stablein	W. Patrick	<u>Letter only</u>
	W. Reamer	B. Meehan	L. Campbell	B. Sagar	CNWRA Directors
	J. Schlueter	J. Greeves	L. Camper	B. Hill	CNWRA Element Managers
	D. DeMarco	A. Campbell	M. Young (OGC)		

D:\GLGP Group\letters\IA\CY-2003\IM-04-22-2003.wpd



Washington Office • Twinbrook Metro Plaza #210
12300 Twinbrook Parkway • Rockville, Maryland 20852-1606

**Magma-Tectonic Interactions in Nicaragua:
The 1999 Seismic Swarm and Eruption of Cerro Negro Volcano**

Peter C. La Femina¹

Rosenstiel School of Marine and Atmospheric Sciences - University of Miami, Miami, FL,
33149-1098, USA

Charles B. Connor²

University of South Florida, Tampa, FL, USA

Brittain E. Hill³

Center for Nuclear Waste Regulatory Analyses,
Southwest Research Institute, San Antonio, TX, USA

Wilfried Strauch⁴ and J. Armando Saballos⁵

Instituto Nicaragüense de Estudios Territoriales, Managua, Nicaragua

Draft of April 16, 2003

To be submitted to:

Journal of Volcanology and Geothermal Research

¹ Corresponding Author; plafemina@rsmas.miami.edu; 305.361.4632

² cconnor@chumal.cas.usf.edu; 813.974.2654

³ bhill@swri.org; 210.522.5155

⁴ wil.gf@ineter.gob.ni; 505.249.1082

⁵ jose.saballos@kcl.ac.uk; 505.249.1082

ABSTRACT

A low energy (VEI 1), small volume (0.001 km^3 DRE) eruption of highly crystalline basalt occurred at Cerro Negro volcano, Nicaragua, August 5–7 1999. This eruption followed three earthquakes (each $\sim M_w$ 5.2) with strike-slip and oblique-slip focal mechanisms, the first of which occurred approximately 11 hours before eruptive activity and within 1 km of Cerro Negro. Surface ruptures formed during these earthquakes extended up to 4 km from Cerro Negro, but concentrated in a left-stepping *en echelon* set south of Cerro Negro. Surface ruptures did not occur within 300 m of the cone, however, three new vents formed along a north-trending alignment on the south flank and base of Cerro Negro. Regional earthquake swarms were located northwest and southeast of Cerro Negro and seismicity was elevated for up to 11 days after the initial event. The temporal and spatial patterns of earthquake swarms, surface ruptures, and the eruption location can be explained using the Hill (1977) model for earthquake swarms in volcanic regions, where an eruption is triggered by tectonically induced changes in the regional stress field. In this model, fractures used for magma ascent are produced by tectonic strain, rather than being initiated by magmatic overpressure. Numerical simulations for the 1999 eruption illustrate that the observed velocities (up to 75 m s^{-1}) and fountain heights (50–300 m) can be achieved by eruption of a magma with little excess magmatic pressure, in response to seismicity and fracturing associated with regional tectonic stress. These observations and models show that 1999 Cerro Negro activity was a tectonically induced small-volume eruption in an arc setting, with the accommodation of extensional strain by dike injection.

Keywords: Cerro Negro volcano, Nicaragua, earthquake swarms, conduit flow

INTRODUCTION

Links between tectonism and magmatism, spanning a wide variety of temporal and spatial scales, are derived from geologic mapping of fault-vent relationships and related criteria (e.g., Lyell, 1830; Kear, 1964; Nakamura, 1977; Parsons and Thompson, 1991; Connor and Conway, 2000; Aranda-Gomez et al., 2003), temporal and spatial patterns of seismicity (Hill, 1977; Linde and Sacks, 1998), and deformation studies (Sigmundsson, et al., 1997; Agustsson, et al., 1999). Extensional terranes with magma productivity may accommodate extensional strain solely through dike injection or a combination of dike injection and normal faulting (Parsons and Thompson, 1991). In volcanic regions with extensional and shear strain, dikes and normal faults form parallel to σ_1 (greatest principal horizontal stress) and strike-slip faults are located on planes oblique (approximately 30°) to σ_1 (Hill, 1977).

The August 1999 eruption of Cerro Negro volcano, Nicaragua, provides an example of how regional tectonic strain likely initiates small volume eruptions. Direct observations of this eruption, coupled with remote sensing, seismicity and deformation data, constrain the timing between tectonic strain and subsequent volcanic eruption. These observations at Cerro Negro are supported by numerical simulations of conduit flow that indicate this eruption required little excess magma pressure, provided that dilation along the dike-fed conduit occurred in response to changes in tectonic (i.e., external) stress, rather than changes in magmatic (i.e., internal) pressure, and support the Hill (1977) model for earthquake swarms in volcanic regions.

TECTONIC SETTING

Cerro Negro is a basaltic cinder cone located at the southern end of a north-northwest-trending alignment of cinder cones, explosion craters, and maars, herein named the Cerro La Mula – Cerro Negro alignment, in the Marabios Range of the Central America Volcanic Arc (CAVA) in western Nicaragua (Figure 1a). This segment of the Marabios Range is bound to the northwest by faults associated with Rota volcano and to the southeast by faults associated with the Las Pilas–El Hoyo volcanic complex and the north-northeast-trending La Paz Centro fault zone (Figure 1a and 1b; van Wyk de Vries, 1993; Cowan et al., 2000). La Femina et al. (2002) suggest that conjugate faulting along north to northeast and north to northwest-trending faults within the CAVA accommodate part of the 14 mm yr^{-1} of trench-parallel dextral shear calculated by DeMets (2001). In this tectonic setting, the former faults are conjugate or anti-Riedel shear faults and the latter are Riedel shear faults. Both fault trends form at approximately 30° to σ_1 and may have a dip-slip component. East-west extension in the CAVA is accommodated by approximately north-trending vent alignments (e.g., the Nejapa-Miraflores alignment; McBirney, 1955a; Walker, 1984; Malavassi and Gill, 1988) and by north-trending normal faults along the CAVA in Nicaragua and Costa Rica (La Femina et al., 2002).

CERRO NEGRO VOLCANO

Cerro Negro first erupted in 1850. Small-volume, low intensity eruptions (23 cumulatively totaling $\sim 0.16 \text{ km}^3$ Dense Rock Equivalent [DRE] and Volcanic Explosivity Index [VEI] 1–3) have constructed the cone of Cerro Negro and surrounding lava flow field at a steady rate (McKnight and Williams, 1997; Hill et al., 1998). The 1999 eruption, which had a very small volume (0.001 km^3 DRE), formed three new vents on the south flank of the cinder cone (Figure 2). This activity was reminiscent of larger volume eruptions in 1929, 1947, 1957, 1968, and 1971, which also produced flank vents. Unlike these earlier eruptions, however, the 1999 eruption did not include any eruptive activity in the main crater of Cerro Negro. Eruptions in 1923, 1947, 1971, and 1992 were substantially more explosive, voluminous, and hazardous (McKnight and Williams, 1997; Hill et al., 1998; Connor et al., 2001).

Cerro Negro's previous eruption, in 1995, consisted of two phases. The first phase began with phreatomagmatic activity and ended with extrusion of a small lava flow in the main crater. During the second phase, several months later, Strombolian activity built a small cone inside the 1992 crater. Lava flows issued from the base of this new cone and flowed to the north down the flanks of the older cone (Figure 2; Connor et al., 1996; Hill et al., 1998). The 1995 eruption culminated with 4 days of violent Strombolian activity that sustained a tephra column 2–2.5-km-high and deposited 0.5 cm of ash 20 km away in the city of León (Hill et al., 1998). The 1995 vent and the 1999 vents form a north-trending

alignment through the main edifice of Cerro Negro, on trend with the Cerro La Mula – Cerro Negro alignment. As described below, the temporal and spatial pattern of earthquake swarms, focal mechanisms of larger earthquakes, and patterns of surface rupturing that accompanied the 1999 eruption further clarify the interplay between tectonic and magmatic processes at Cerro Negro.

AUGUST 1999 SEISMIC AND ERUPTIVE ACTIVITY

Seismic activity

The 1999 activity began with a M_L 4.0 earthquake at Cerro Negro volcano at 04:19 GMT (22:19 Local - August 4, 1999) on August 5, 1999 (INETER, 1999). Over the next three hours, two M_w 5.2 (M_s 4.6 and M_s 4.5) and one M_w 5.1 (M_s 4.6) earthquakes occurred east and southeast of Cerro Negro (Figure 1a; INETER, 1999; Dziewonski et al., 2000). The centroid moment tensor solutions for these earthquakes indicate oblique, sinistral slip on northeast-trending fault planes, or oblique, dextral slip on northwest-trending fault planes (Figure 1a; INETER, 1999; Dziewonski et al., 2000), which is consistent with the pattern of faulting in this area (van Wyk de Vries, 1993; Cowan et al., 2000; La Femina et al., 2002). Following these larger earthquakes, regional microseismicity increased and earthquake swarms occurred northwest and southeast of Cerro Negro, at the southeastern edge of Rota volcano and the northwestern flank of Las Pilas–El Hoyo volcanic complex, respectively (Figure 1b). In addition, earthquakes associated with the eruption were clustered around the Cerro Negro eruptive vents and along the Cerro La Mula–Cerro Negro alignment. These patterns of microseismicity continued through August 6, 1999.

On August 7, an earthquake swarm occurred within the La Paz Centro fault zone (Figure 1b). This swarm began at 7:42 GMT with a M_L 4.6 earthquake and was followed by approximately 32 earthquakes ranging between M_L 1.1 and 3.7. On August 8, approximately 25 similar magnitude earthquakes occurred. Ground shaking associated with this swarm caused building collapse in the town of Puerto Momotombo. Beginning on August 9, seismicity within the Marabios Range decreased rapidly to near background levels by August 18 (Figure 3).

August 5-7, 1999 eruption

Three new volcanic vents formed along a north-trending alignment south of Cerro Negro early on August 5, approximately 11 hours after the first earthquake (Figure 2). Thermal anomalies in GOES mid-infrared radiance data show the eruption began within 15 minutes of 9:41 GMT (Harris et al., 2000). These new vents formed adjacent to the 1968 Cristo Rey vent, in an area previously characterized by above background ^{222}Rn soil-gas flux thought to be associated with a fault (Connor et al., 1996). The first vent formed on the flank of Cerro Negro and was a phreatic explosion crater with a diameter of approximately

30 m (Figure 2). This vent produced little or no juvenile material. An approximately 200-m-long fissure then formed to the south of this vent. Fire fountaining along this fissure later coalesced into two additional vents. Eruption from these vents constructed two new scoria cones to heights of 40 m by August 6, along with two small-volume lava flows that breached and rafted the flanks of the scoria cones. This activity is similar to that described for the 1968 eruption and formation of the parasitic cone Cristo Rey, which was partially buried by the 1999 vents (Viramonte and DiScala, 1970). Seismic activity during this time consisted of volcano-tectonic tremors of approximately M_w 3.0 occurring about every 4 minutes. Most tephra dispersal ceased by 18:00 on August 6, with lava effusion from the scoria cones and small pyroclastic fountains continuing until around 06:00 on August 7. In total, the 1999 eruption lasted 2 days.

The eruption was observed from a site approximately 1 km southeast of Cerro Negro. Tephra column heights ranged from 2 to 2.5 km during August 5–6, 1999. Winds from the east deflected the tephra column beginning about 200 m above the vent, which is characteristic of a weak tephra plume. Tephra columns were produced by eruptions from both vents, however, the input from each vent varied through time. Incandescent fountain heights from both vents ranged from 50–300 m, and possibly up to 500 m, between August 5 and 7. The rate of fountaining decreased over time from once per second on August 5 to once per several minutes on August 7, until the eruption ceased.

Dispersed tephra deposits (Figure 2) represent the eruption of only $5 \times 10^4 \text{ m}^3$ (DRE) of basaltic magma. Based on detailed surveys of the 1999 deposits (Figure 2), $6 \times 10^5 \text{ m}^3$ (DRE) of basaltic magma erupted as lavas and $4 \times 10^5 \text{ m}^3$ (DRE) as scoria cones. In total, 0.001 km^3 of basaltic magma was erupted. Average mass-flow rates for the 1999 eruption were $0.5 \text{ m}^3 \text{ s}^{-1}$ for tephra and $4 \text{ m}^3 \text{ s}^{-1}$ for lava, which are comparable to the longer-duration 1995 eruption (Hill et al., 1998).

Basalt from the 1999 eruption is compositionally similar to 1995 basalt. Modal mineral abundances (Table 1) are within 1 standard deviation of analytical uncertainty for the two eruptions, with the exception of a slightly increased clinopyroxene abundance in 1999 basalt. Most geochemical abundances for 1999 and 1995 basalt are within 1 standard deviation of analytical uncertainty (Table 2). However, small but significant variations occur in CaO, K_2O , Cr and Ni abundances. Simple least-squares mass balance models show that these geochemical variations are consistent with the accumulation of 3 percent each clinopyroxene and plagioclase, along with 2 percent olivine, in the 1999 basalt relative to 1995 basalt. Small amounts of intraeruption and intereruption crystal accumulation or fractionation are characteristic of the Cerro Negro basaltic magma system (Walker and Carr, 1986; McKnight, 1995; Hill et al., 1998). Based on these relationships, the small-volume 1999 basalt most likely represents a residual magma from the 1995 eruption, which retained sufficient mass and heat to allow phenocrysts to migrate into the erupted region of the magma system (i.e., Carr and Walker, 1987). Alternatively, the observed compositional variations may

reflect continued withdrawal from a slightly zoned shallow magma system that has erupted sporadically since about 1971.

We classify this eruption as mild strombolian (VEI 1) based on the volume of tephra and range in column heights. The velocities of pyroclasts leaving the vent calculated from observed fountain heights were 30 m s^{-1} (50 m fountain) to 75 m s^{-1} (300 m fountain). Volcanic bombs also were found up to 300 m from the vents, indicating initial pyroclast velocities of up to 65 m s^{-1} .

Fractures and surface ruptures formed during August 1999 activity

Surface ruptures formed during August 1999 seismic and volcanic activity in the area south and southwest of Cerro Negro. We mapped the position of surface ruptures with a real-time kinematic differential GPS (DGPS), with horizontal and vertical accuracies of $\pm 2 \text{ cm}$ and $\pm 10 \text{ cm}$ (2 sigma), respectively. Although we believe we have mapped all major fractures, it is possible that we missed some smaller fractures due to patches of dense vegetation. A prominent, north-northwest-trending fracture system, with up to 0.9 m of dilation, formed beginning about 500 m south of Cerro Negro (Figure 2). Three >100-m-long segments along this fracture system indicate a possible left-stepping *en echelon* pattern. At a distance of 1 km south of Cerro Negro, the fracture system changed to a northwesterly strike and intersected the Las Pilas-El Hoyo volcano complex (Figure 2). At this location, anastomosing fractures formed a zone 15 m wide, with up to 0.5 m vertical offset between blocks and 0.5–0.9 m total dilation (Figures 2 and 4). In this area the fracture system intersected a pre-existing, shallow geothermal system, and 40° – 90° C vapor emanated from a 100-m-long segment. This activity (i.e., fracturing and vapor emanation) is similar to more vigorous activity at Las Pilas volcano in 1952 (McBirney, 1955b) and Cerro Negro in 1968 (Viramonte and DiScala, 1970). The 1999 fracture system continued along strike across the northern flank of an unnamed cone west of Las Pilas, but also splayed out normal to the slope, forming slumps.

Two >150-m-long north-northwest-trending fracture systems also formed approximately 300 m southeast of the new vents (Figure 2). Total dilation measured across this system, however, was only 17 cm. Approximately 4 km south-southwest of Cerro Negro we also measured 11 cm of down-to-the-east displacement along an approximately 100-m-long, north-trending set of fractures. North-trending surface ruptures were also observed in the town of Rota 5 km west-northwest of the volcano (Figure 1a). Formation of these surface ruptures caused building damage in Rota.

The 1999 eruption of Cerro Negro differed from 1968–1995 eruptions in several important ways. First, the eruption was entirely outside the main vent. Although other eruptions (e.g., 1968) produced flank vents and fissures, activity also occurred in the main vent. Second, development of fractures as mapped in 1999 did not occur in 1992 or 1995. Fractures were reported south of Cerro Negro in 1968 (Viramonte and

DiScala, 1970), but were not mapped or described in detail. Third, there is no record of local large magnitude earthquakes preceding 1968–1995 eruptions. Fourth, the 1999 eruption was much smaller in volume than these previous eruptions. Cumulatively, these observations indicate a more effusive eruptive style occurred in 1999 than in the five previous Cerro Negro eruptions.

DISCUSSION

The August 1999 regional earthquake swarm within the Marabios Range and eruptive activity at Cerro Negro reveal that shear and extensional strain were accommodated by a combination of fault slip and dike injection during a single event. This suggests that magma ascent and subsequent dike injection may have occurred primarily in response to changes in regional tectonic stress. Hill (1977) presented a model for earthquake swarms in volcanic regions and suggested that dike injection could occur in response to changes in the regional stress field. Several of our observations agree with this model, including: 1) the three $>M_w$ 5.0 earthquakes that preceded eruptive activity, which produced strike-slip or oblique-slip focal mechanisms, 2) dike injection and new vents, which formed parallel to the greatest horizontal principal stress σ_1 , 3) regional earthquake swarms, which were located on planes oblique to σ_1 , and 4) seismic activity throughout the Marabios Range, including the La Paz Centro fault zone seismic swarm, which was elevated for up to 11 days after the main events and not exclusively related to areas of dike injection.

In the Hill (1977) earthquake swarm model, there are two processes considered that cause earthquake swarms. The first process involves an increase in magmatic pressure P_f such that $P_f > \sigma_3$. This allows for dike growth and the formation of earthquake swarms by shear failure along planes oblique to the dike. The second process involves changes in the regional stress difference $\sigma_1 - \sigma_3$, which permits fracture dilation and allows for dike injection and the subsequent formation of an earthquake swarm.

The nature of volcanic eruptions helps differentiate these two processes. In the former case, excess magma pressure drives dike injection and ascent. This magma pressure, on the order of 10 MPa above lithostatic, can be produced by the rapid rise of magma from depth. Alternatively, overpressure might be produced by seismicity (Sahagian and Proussevitch, 1992; Linde et al., 1994; Linde and Sacks, 1998). Regardless of the controlling process, this excess pressure should result in comparatively high flow rates at the surface. In contrast, consider magma initially in near buoyant equilibrium with the crust, which is consistent with mineralogical data that indicates the 1999 magma is likely a residual of 1995 magma. Under these conditions the magma has little or no excess pressure (e.g., < 1 MPa pressure in excess of lithostatic). If magma density is slightly less than the mean density of the overlying crust (Lister and Kerr, 1991), buoyancy forces are insufficient in most conditions of deviatoric stress to initiate the propagation of a fracture through the crust and drive dike injection. That is, the tangential stress imparted by the magma on

the overlying rock is insufficient to initiate hydrofracturing and permit magma ascent. For such underpressured magmas, fracturing is necessarily initiated by tectonic strain, such as the initial $M_w > 5.0$ earthquakes and subsequent regional seismicity at Cerro Negro. In this event, fractures formed parallel to σ_1 and may have dilated in response to predominantly left-lateral strike-slip faulting. Because of this tectonically induced fracturing, the tangential stress required to initiate magma ascent was likely lower than in previous eruptions. If this conceptual model for the 1999 eruption is correct, magma ascent and eruption would have initiated at lower magmatic pressures than otherwise possible.

The character of eruptions and relationship to magma pressure at depth is investigated using a 1D steady-state model of conduit flow. This model is used to compare eruption conditions for a magma with little or no excess pressure to one where excess pressure is present. Our model for magma ascent is based on the numerical approach developed by Woods (1995) (also see Mader, 1996; Jaupart, 2000) for a low volatile basaltic magma. This approach solves for pressure and flux conditions along the flow path, using a finite difference approximation that is isothermal, assumes magma and gas phases are incompressible, and contains a bulk approximation to the equation of state (Sparks et al., 1997). Flow conditions are assumed to be steady-state, and equations for continuity and momentum are solved iteratively using the Runge-Kutta method (Press et al., 1990).

The magma is assumed to be volatile poor (0.5–1.5 weight percent), relative to the 1992 and 1995 Cerro Negro magmas. This could be possible through degassing of common or similar parent magma at shallow crustal levels (Roggensack et al., 1997), which is consistent with observed petrological relationships. Viscosity (on the order of 100 Pa s) and temperature (1100° C) are held constant in our model. A 0.5 m dike width and 10 m² vent aperture are used in this model.

Results of the simulation of flow conditions during ascent using this model are shown for initial gas contents of 0.5, 1, and 1.5 weight percent water in the magma (Figure 5). Note that the ascent velocities for magma from depth are reasonably low (0.5–4 m s⁻¹) and that the exit velocities of the gas and pyroclast mixture at the vent vary from 35 m s⁻¹ to 75 m s⁻¹, in agreement with observations made during the pyroclastic phase of the 1999 eruption. These exit velocities and conduit geometry give mass flow rates of 1.5×10^4 to 1×10^5 kg s⁻¹, in reasonable agreement with the observed fire-fountain heights of 50–300 m and total volume of the 1999 deposit. These model results are not sensitive to magma reservoir depth, as long as the reservoir is so deep that volatiles do not exsolve. In contrast, if initial magma pressures of 10 MPa above lithostatic are assumed, corresponding to a magma overpressure sufficient to drive a dike through the crust, then modeled flow rates at the surface are higher, on the order of $2\text{--}4 \times 10^5$ kg s⁻¹. Although these flow rates are approximately double those estimated from direct observations of the 1999 eruption, they are comparable to flow rates calculated for the 1992 Cerro Negro eruption (Hill et al., 1998). This modeling

relationship suggests that the 1992 eruption may have been controlled by buoyant rise of magma from depth (i.e., higher magma pressures) or higher initial volatile contents, relative to the 1999 eruption.

This model is a simplification of a complex eruption process. For example, pulsing fire-fountains that occurred during the eruption likely indicate the development of annular flow in the conduit (e.g., Vergnolle and Jaupart, 1986), and a breakdown in the assumption that a single equation of state captures the flow process. Nonetheless, the most energetic phase of the 1999 eruption appears well bounded by the model.

We conclude from these calculations and field observations that the 0.5–1.0 m of dilation that occurred across the Cerro Negro region in August, 1999, appears sufficient to initiate the eruption of this low-volatile magma, which otherwise might have cooled and crystallized in the shallow subsurface without eruption. The short duration of eruptive activity and the fact that the eruption was outside the main vent also supports tectonically induced dilation of the conduit, rather than dilation by magmatic overpressure. A dike width of 0.5 m, comparable to the fracture dilation we measured 1 km from the cone, would solidify against flow in approximately 2 days via conductive cooling (Bruce and Huppert, 1989), again correlating well with observations of this eruption. The fact that the eruption did not occur through the main vent also is consistent with low magmatic pressures (Gudmundsson et al., 1992).

CONCLUSIONS

The 1999 eruption of Cerro Negro volcano closely followed several tectonic earthquakes and coincided with a regional earthquake swarm. The VEI 1 eruption was most notable for its small volume, lack of activity from the central vent of Cerro Negro, and effusion of highly crystalline basalt. Low eruption rate, association with a regional seismic swarm, and results of numerical simulation of the eruption suggest that this magma may have erupted as a consequence of tectonic strain and seismicity, rather than in response to internal magma pressure. Therefore, 1999 Cerro Negro activity is an excellent example of a tectonically induced small-volume eruption in an arc setting and for the accommodation of extensional strain by dike injection.

ACKNOWLEDGMENTS

Careful reviews by Dave Hill, Alexander McBirney, Steve Sparks, Tim Dixon, John Stamatakis, Wesley Patrick, and an anonymous reviewer improved the manuscript and are greatly appreciated. Part of this work was performed by the Center for Nuclear Waste Regulatory Analyses (CNWRA) for the U.S. Nuclear Regulatory Commission (NRC) under Contract Nos. NRC-2-97-009 and NRC-02-02-12. The activities reported here were performed on behalf of the NRC Office of Nuclear Material Safety and Safeguards, Division of Waste Management. This work is an independent product of the CNWRA and does not necessarily reflect the views or regulatory position of the NRC. PCL was also supported by a NASA Florida Space Grant Fellowship and CC was also supported by a grant from the National Science Foundation (EAR-0130602).

REFERENCES

- Agustsson, K., Linde, A.T., Stefansson, R., and Sacks, S., 1999. Strain changes for the 1987 Vatnafjoll earthquake in south Iceland and possible magmatic triggering. *J. Geophys. Res.*, 104: 1151-1161.
- Aranda-Gomez, J.J., J.F. Luhr, T.B. Housh, C. B. Connor, T. Becker, and C.D. Henry, 2003. Synextensional, Plio-Pleistocene eruptive activity in the Camargo volcanic field, Chihuahua, México. *Geol. Soc. of America Bull.*, 115 (3): 298-313.
- Bruce, P.M., and H. Huppert, 1989. Thermal control of basaltic fissure eruptions. *Nature*, 342: 665-667.
- Carr, M.J., and J.A. Walker, 1987. Intra-eruption changes in composition of some mafic to intermediate tephra in Central America. *J. Volcanol. Geotherm. Res.*, 33: 147-159.
- Connor, C.B. and Conway, F.M., 2000. Volcanic fields. In: H. Sigurdsson (Editor), *Encyclopedia of Volcanoes*. Academic Press, San Diego, pp 331-343.
- Connor, C.B., B. Hill, P. La Femina, M. Navarro, and M. Conway, 1996. Soil ^{222}Rn pulse during the initial phase of the June-August 1995 eruption of Cerro Negro, Nicaragua. *J. Volcanol. Geotherm. Res.*, 73: 119-127.
- Connor, C.B., B.E. Hill, B. Winfrey, N.M. Franklin, and P.C. La Femina, 2001. Estimation of volcanic hazards from tephra fallout. *Nat. Haz. Rev.*, 2: 33-42.
- Cowan, H., Machette, M.N., Amador, X., Morgan, K.S., Dart, R.L., and Bradley, L., 2000. Map and database of Quaternary faults in the vicinity of Managua, Nicaragua: U.S. Geological Survey Open-File Report 00-437, 15 p.
- DeMets, C., 2001. A new estimate for present-day Cocos-Caribbean plate motion: Implications for slip along the Central American volcanic arc. *Geophys. Res. Lett.*, 28 (21): 4043-4046.

- Dziewonski, A.M., Ekstrom, G., and Maternovskaya, N.N., 2000. Centroid-moment tensor solutions for July-September 1999. *Phys. Earth Plan. Int.*, 119 (3-4): 311-319.
- Gudmundsson, A. and 11 others, 1992. The 1991 eruption of Hekla, Iceland. *Bull. Volc.*, 54: 238-246.
- Harris, A., Flynn, L., and Pilger, E., 2000. *Bulletin of the Global Volcanism Network*, Smithsonian Institution, Washington, D.C.
- Hill, B.E., Connor, C.B., Jarzempa, M., La Femina, P.C., M. Navarro, and W. Strauch, 1998. 1995 eruptions of Cerro Negro volcano, Nicaragua, and risk assessment for future eruptions. *Geol. Soc. of America Bull.*, 110: 1231-1241.
- Hill, D.P., 1977. A model for earthquake swarms. *J. Geophys. Res.*, 82: 1347-1352.
- INETER, Boletín of Sismológico Mensual "Sismos y Volcanes de Nicaragua," Agosto, 1999.
- Jaupart, C., 2000. Magma ascent at shallow levels. In: H. Sigurdsson (Editor), *Encyclopedia of Volcanoes*. Academic Press, San Diego, pp 237-248.
- Kear, D., 1964. Volcanic alignments north and west of New Zealand's central volcanic region. *New Zealand J. of Geol. Geophys.*, 7: 24-44.
- La Femina, P.C., Dixon, T.H., Strauch, W., 2002. Bookshelf faulting in Nicaragua. *Geology*, 30 (8): 751-754.
- Linde, A.T., Sacks, I.S., 1998. Triggering of volcanic eruptions. *Nature*, 395 (6705): 888-890.
- Linde, A.T., Sacks, I.S., Johnston, M.J.S., Hill, D.P., and Bilham, R.G., 1994. Increased pressure from rising bubbles as a mechanism for remotely triggered seismicity. *Nature*, 371: 408-410.
- Lister, J.R., and R.C. Kerr, 1991. Fluid mechanical models of crack propagation and their application to magma transport in dykes. *J. Geophys. Res.*, 96: 10,049-10,077.
- Lyell, C., 1830. *Principles of Geology: Volume 1*. reprinted 1990 by University of Chicago Press, Chicago.
- Mader, M.H., 1996. Conduit flow and fragmentation, in: J.S. Gilbert and R.S.J. Sparks (Editors) *The Physics of Explosive Volcanic Eruptions*. Geological Society, London, Special Publications. 145, pp 51-72.
- Malavassi, E., and Gill, J.B., 1988. Aguas Zarcas cones, unfractionated basalts behind the volcanic field in central Costa Rica. *Eos, Transactions, American Geophysical Union*, 69 (44): 1493.
- McBirney, A.R., 1955a. The origin of the Nejapa pits near Managua, Nicaragua. *Bull. Volcanol.*, 17: 145-154.
- McBirney, A.R., 1955b. Thoughts on the eruptions of the Nicaraguan volcano Las Pilas. *Bull. Volcanol.*, 17: 113-117.
- McKnight, S.B. 1995. *Geology and Petrology of Cerro Negro Volcano, Nicaragua* [M.S. Thesis]: Tempe, AZ: Arizona State University, pp 132.

- McKnight, S.B., and Williams, S.N., 1997. Old cinder cone or young composite volcano?: The nature of Cerro Negro, Nicaragua. *Geology*, 25: 339-342.
- Nakamura, K., 1977. Volcanoes as possible indicators of tectonic stress orientation – principles and proposal. *J. Volcanol. Geotherm. Res.*, 2: 1-16.
- Parsons, T. and Thompson, G.A., 1991. The role of magma overpressure in suppressing earthquakes and topography: Worldwide examples. *Science*, 253: 1399-1402.
- Press, W.H., B.P. Flannery, S.A. Teukolsky, and W.T. Vetterling, 1990. *Numerical Recipes, the Art of Scientific Computing*. Cambridge University Press, Cambridge, 708 pp.
- Roggensack, K., Hervig, R.L., McKnight, S.B., Williams, S.N., 1997. Explosive basaltic volcanism from Cerro Negro volcano, Influence of volatiles on eruptive style. *Science*, 277: 1639-1642.
- Sahagian, D.L., and Proussevitch, A.A., 1992. Bubbles in volcanic systems. *Nature*, 359: 485.
- Sigmundsson, F., Einarsson, P., Rognvaldsson, S.T., Foulger, G., Hodgkinson, K.M., and Thorbergsson, G., 1997. The 1994-1995 seismicity and deformation at the Hengill triple junction, Iceland: Triggering of earthquakes by minor magma injection in a zone of horizontal shear stress. *J. Geophys. Res.*, 102: 15,151-15,161.
- Sparks, R.S.J., Bursik, M.I., Carey, S.N., Gilbert, J.S., Glaze, L.S., Sigurdsson, H., and Woods, A.W., 1997. *Volcanic Plumes*, John Wiley and Sons, New York.
- van Wyk de Vries, B., 1993. *Tectonics and magma evolution of Nicaraguan volcanic systems [PhD thesis]: Milton Keynes, U.K., The Open University*, pp 328.
- Vergnolle, S., and Jaupart, C., 1986. Separated two-phase flow and basaltic eruptions. *J. Geophys. Res.* 91(B12): 12,842-12,860.
- Viramonte, J.G., and DiScala, L., 1970. Summary of the 1968 eruption of Cerro Negro, Nicaragua. *Bull. Volc.*, 34: 347-351.
- Walker, J.A., 1984. Volcanic rocks from the Nejapa and Granada cinder cone alignments, Nicaragua, Central America. *J. Petrol.*, 25 (2): 299-342.
- Walker, J.A., and M.J. Carr. 1986. Compositional variations caused by phenocryst sorting at Cerro Negro volcano, Nicaragua. *Geol. Soc. Am. Bull.*, 97: 1156-1162.
- Woods, A.W., 1995. The dynamics of explosive volcanic eruptions. *Rev. of Geophys.*, 33: 495-530.

Figure Captions.

Figure 1A. Geologic setting of Cerro Negro volcano (CN) in the Marabios Range of northwestern Nicaragua (see inset), including the volcanic complexes of Rota, El Hoyo, and Momotombo volcanoes. Faults (solid thick lines) from van Wyk de Vries (1993) and Cowan et al. (2000). Black stars are epicenter locations for the three M_w 5.1–5.2 earthquakes that preceded the eruption, with focal mechanisms from Dziewonski et al. (2000). Epicenter of the M_L 4.6 earthquake that started the La Paz Centro earthquake swarm on August 7 also is shown in black star. Hexagons indicate CN, Cerro La Mula (CLM) and Las Pilas (LP) volcanoes. Rectangles indicate the towns of Rota (R), Puerto Momotombo (PM) and La Paz Centro (LPC). Topographic contour interval is 100 m.

Figure 1B. Distribution of earthquakes during the seismic swarms of August, 1999. Seismic data are from the INETER seismic network. Hexagon indicates Cerro Negro volcano, white stars are epicenter locations from Figure 1a.

Figure 2. Topographic map of Cerro Negro and products of the August 5–8, 1999 eruption. Topography mapped with differential Global Positioning System and interpolated on a 50 m grid, contour interval is 20 m. Surface fractures mapped in thick black lines, 1999 tephra deposit isopachs (dashed lines) shown in centimeters. 1995 vent located in central crater of main cone. Coordinates in Universal Transverse Mercator, Zone 16, NAD-27 spheroid. Black box indicates area studied for Figure 4.

Figure 3. Daily earthquake count within the Marabios Range between August 1 and August 31, 1999 (INETER, 1999). Earthquakes with magnitudes greater than M 1.1 are plotted. The eruption on August 5 and La Paz Centro seismic swarm on August 7 and 8 clearly stand out.

Figure 4. Cumulative displacement across the 1999 fracture zone, measured along seven scan lines located 10 m apart and 1 km south of Cerro Negro. Cumulative dilation in this area varied from 60–90 cm.

Figure 5. Models of magma velocity in a conduit versus depth, for magmas with initial gas contents of 0.005, 0.01, and 0.015 weight fraction water. These initial conditions produce a range of muzzle velocities (v) and fluxes (Q) consistent with observations made during the 1999 Cerro Negro eruption.

Table 1. Modal mineral abundances for Cerro Negro basalt.

Component	1995 lava	1999 lava
Samples	5	4
Points/sample	1200 \pm 200	1600 \pm 300
Groundmass*	56 \pm 3	59 \pm 3
Plagioclase	34 \pm 3	26 \pm 4
Olivine	5.2 \pm 1.3	5.3 \pm 1.3
Augite	4.4 \pm 1.7	9.3 \pm 3.0
Opakes	0.4 \pm 0.3	0.4 \pm 0.1
(Vesicles)	(11 \pm 9)	(12 \pm 8)

Note: Modes as area percent, vesicle free. Vesicle abundances shown in parentheses for reference.

*Groundmass refers to crystals smaller than 0.1 mm and glass.

Table 2. Cerro Negro basalt analyses.

	1995 main lava	1999 early lava	1999 late scoria	Uncertainty $\pm 1\sigma$
SiO ₂	50.0	49.5	49.2	0.3
TiO ₂	0.796	0.767	0.734	0.004
Al ₂ O ₃	18.73	18.31	18.04	0.19
FeO ^T	10.27	10.41	10.30	0.21
MnO	0.191	0.192	0.190	0.001
MgO	5.48	6.31	6.79	0.05
CaO	11.50	11.79	12.07	0.12
Na ₂ O	2.39	2.22	2.16	0.17
K ₂ O	0.49	0.43	0.41	0.01
P ₂ O ₅	0.114	0.099	0.094	0.005
Total*	99.78	99.22	99.70	
Sc [§]	39	45	45	8
V [†]	315	319	310	6
Cr [§]	45	57	74	5
Ni [†]	16	23	22	2
Zn [†]	73	77	71	4
Ga [†]	17	19	16	2
Pb [§]	1.7	1.6	1.6	0.2
Rb [§]	7.9	7.4	7.2	0.6
Sr [§]	423	415	413	8
Cs [§]	0.38	0.34	0.33	0.03
Ba [†]	388	356	324	19
La [§]	3.5	3.2	3.1	0.7
Ce [§]	7.5	6.8	6.7	0.6
Pr [§]	1.19	1.10	1.06	0.08
Nd [§]	6.2	5.7	5.4	0.6
Sm [§]	2.1	1.9	1.9	0.2
Eu [§]	0.86	0.82	0.81	0.05
Gd [§]	2.7	2.5	2.5	0.3
Tb [§]	0.49	0.45	0.44	0.05
Dy [§]	3.0	2.8	2.7	0.2
Ho [§]	0.65	0.60	0.58	0.05
Er [§]	1.8	1.7	1.6	0.1
Tm [§]	0.26	0.24	0.23	0.02
Yb [§]	1.6	1.5	1.5	0.1
Lu [§]	0.26	0.24	0.23	0.02
Y [§]	16.6	15.9	15.3	0.8
Zr [†]	40	38	34	1
Hf [§]	1.1	1.0	1.0	0.1
Nb [§]	1.17	1.08	1.04	0.09
Ta [§]	0.08	0.07	0.07	0.01
Th [§]	0.37	0.30	0.29	0.06
U [§]	0.29	0.25	0.22	0.04

Note: Major element analyses by X-ray fluorescence, normalized 100%, volatile free, total Fe as FeO^T.

*Original analytical total.

[†]Analysis by X-ray fluorescence, parts per million.

[§]Inductively coupled plasma mass spectrometer, parts per million.

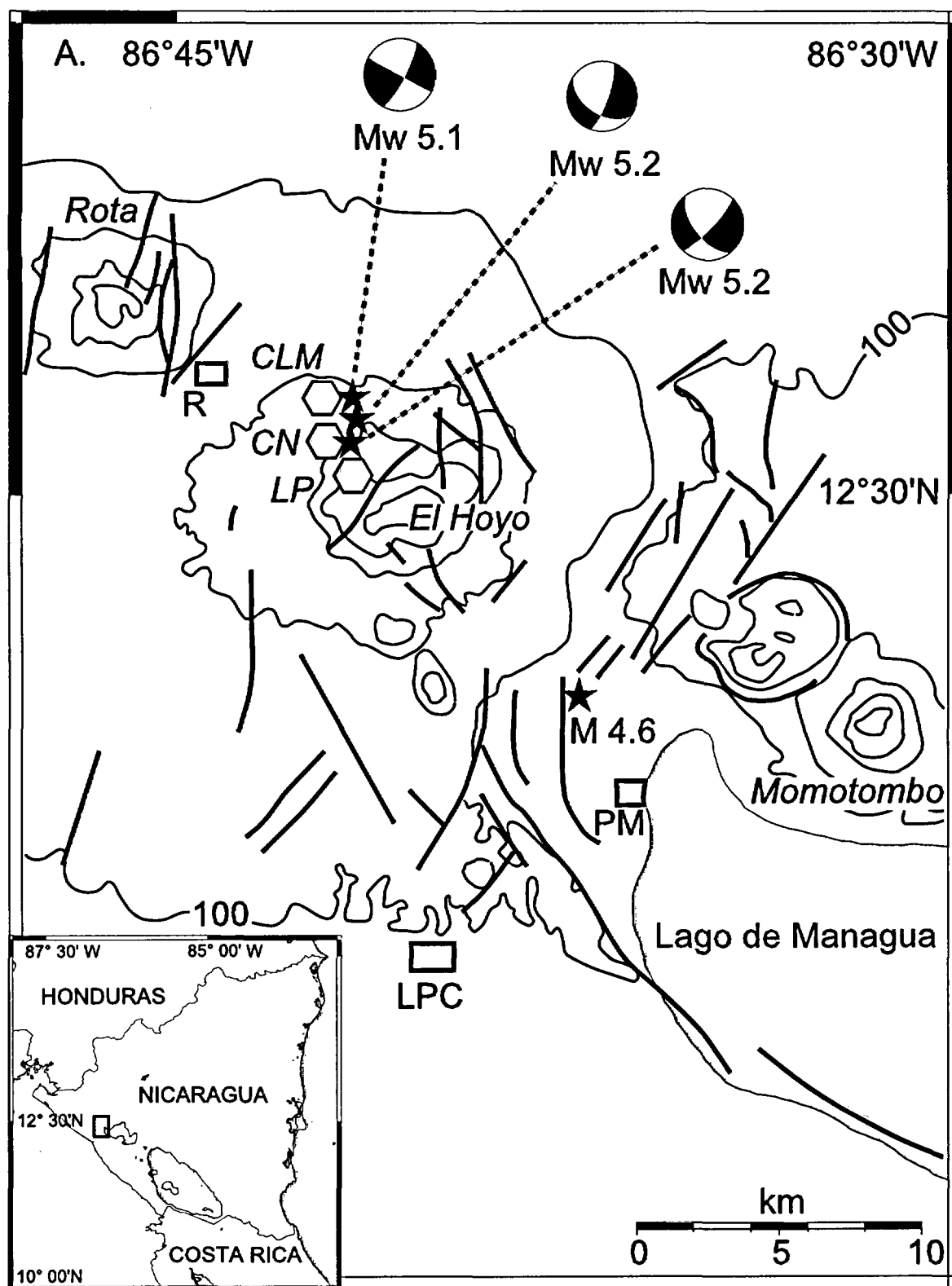


Figure 1a - La Femina et al.

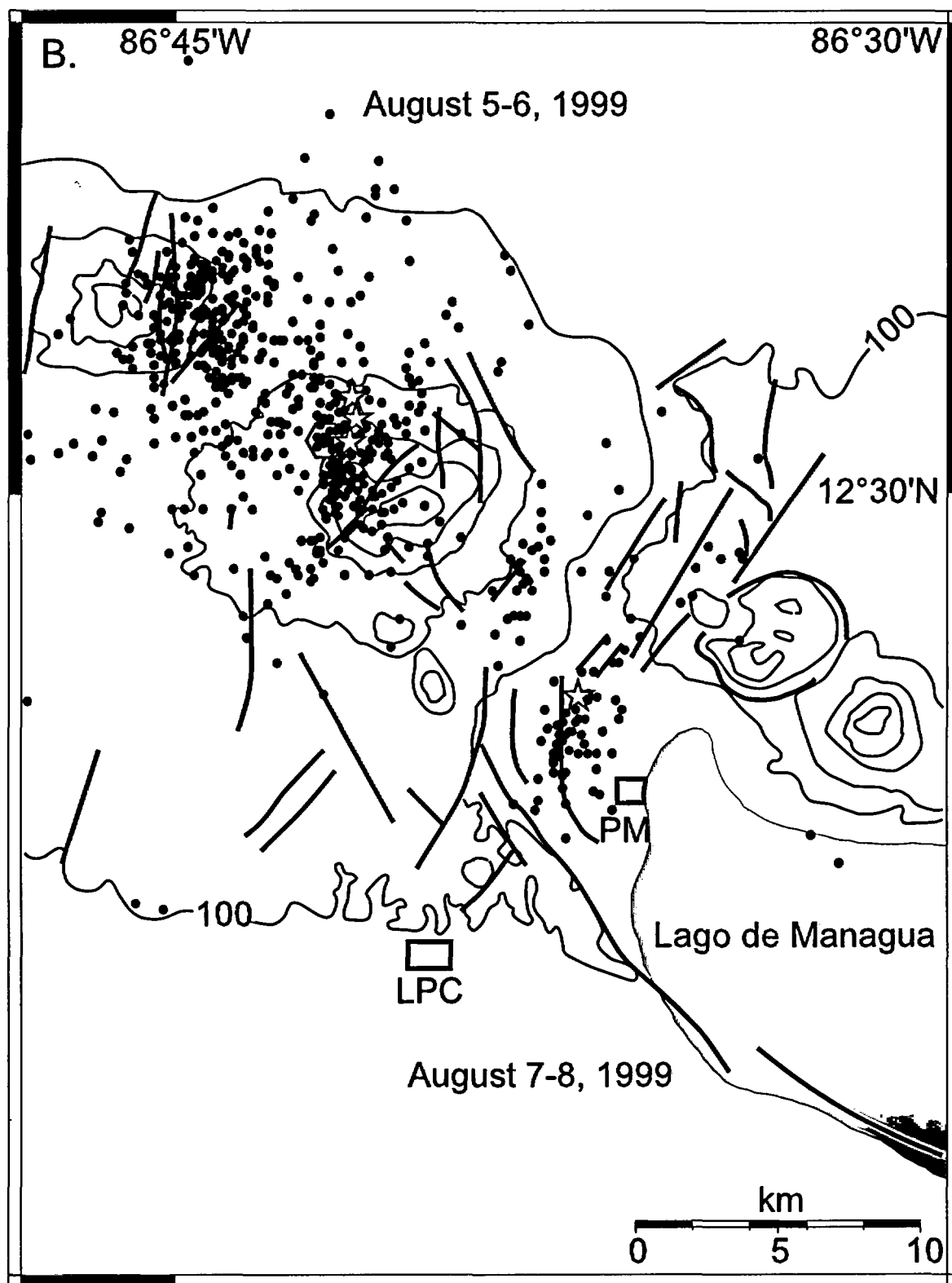


Figure 1b - La Femina et al

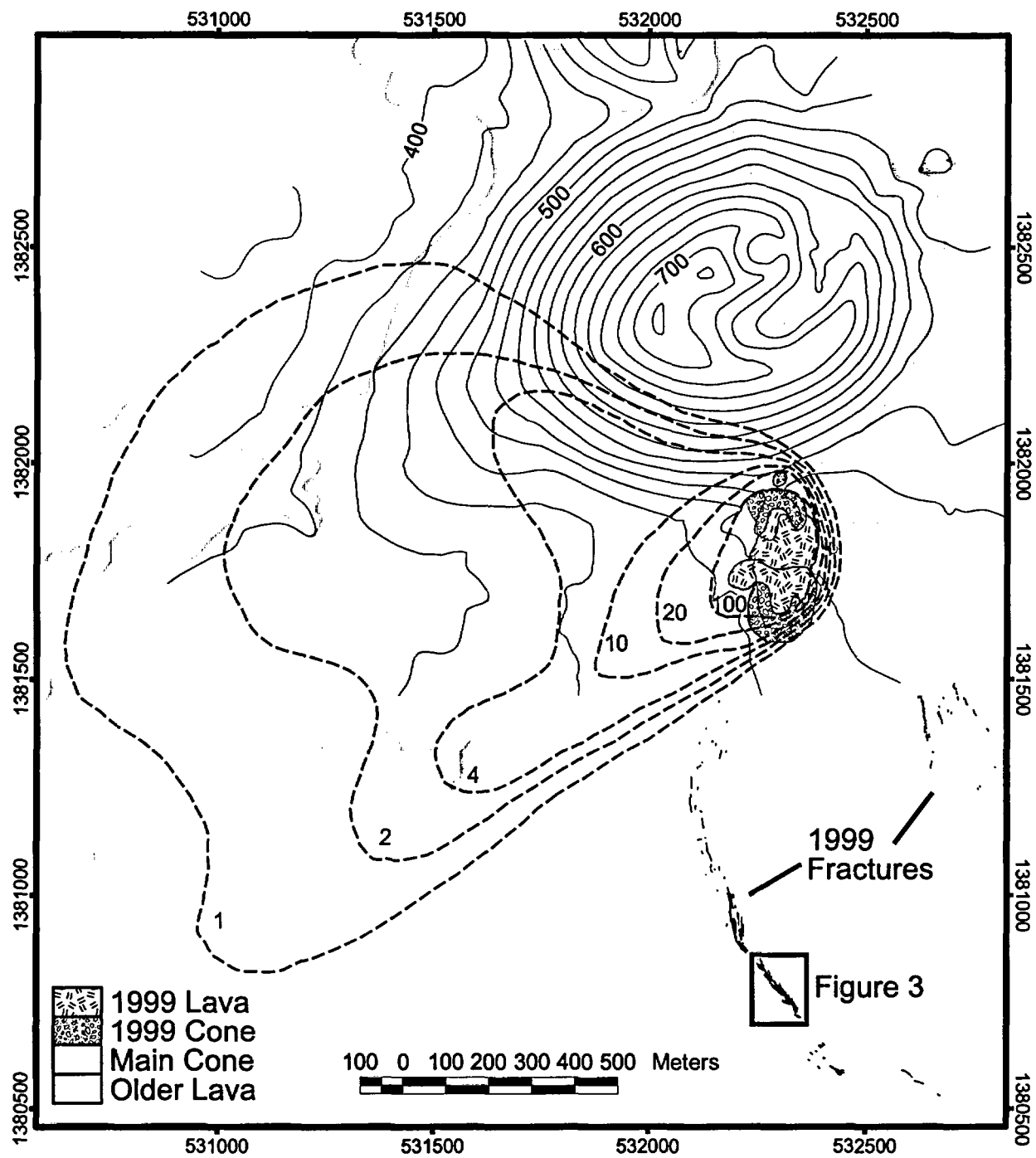


Figure 2 - La Femina et al.

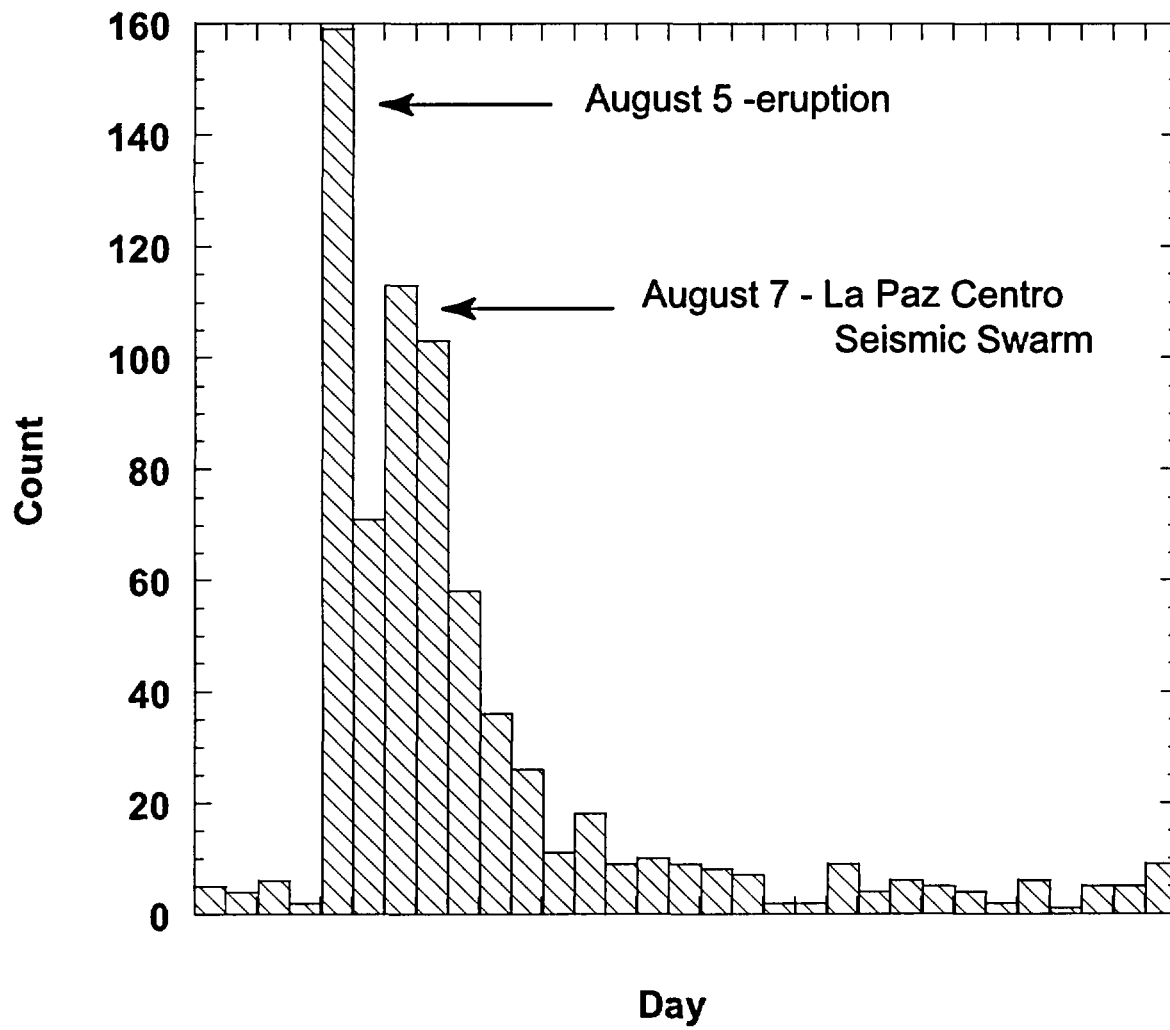


Figure 3. La Femina et al

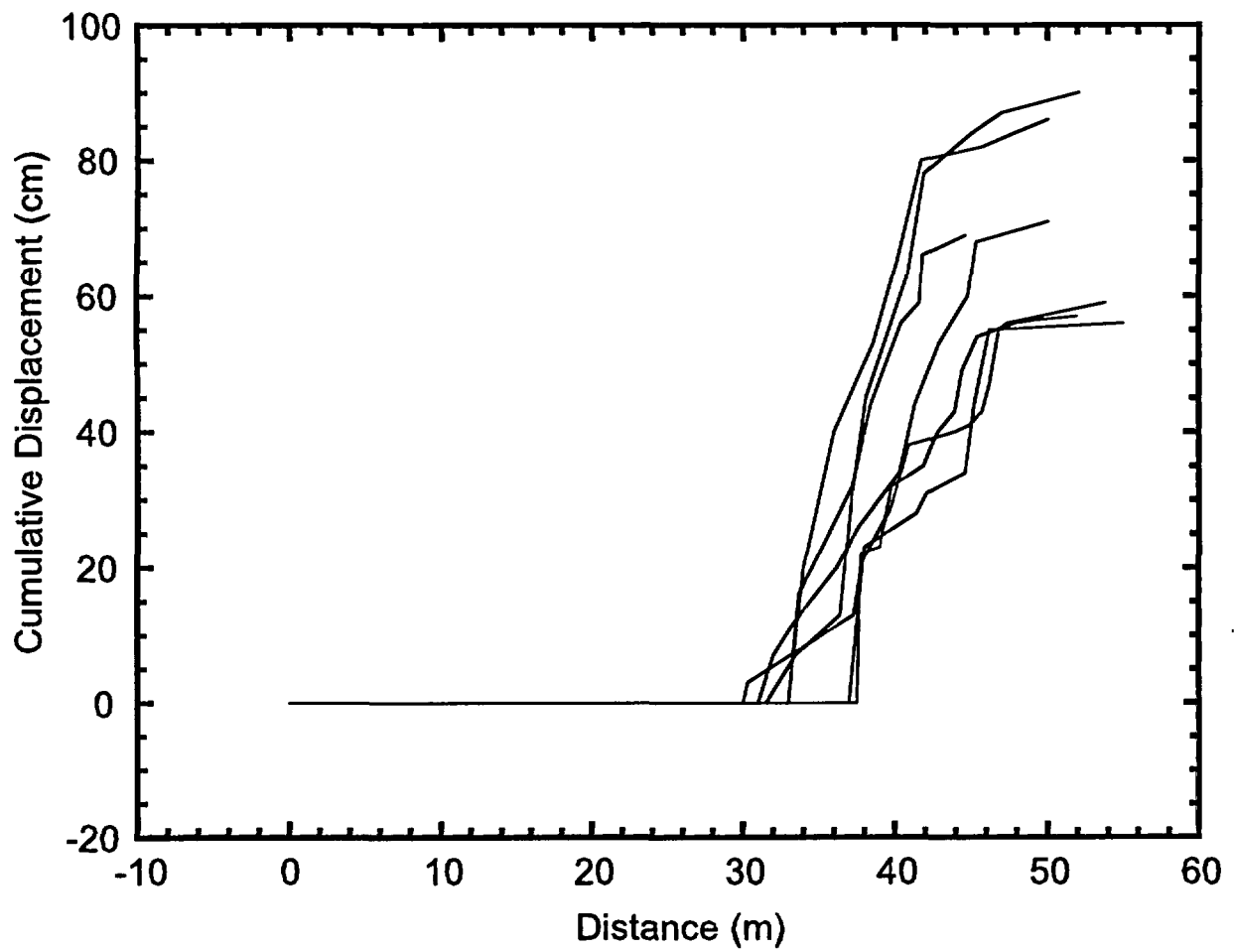


Figure 4 - La Femina et al

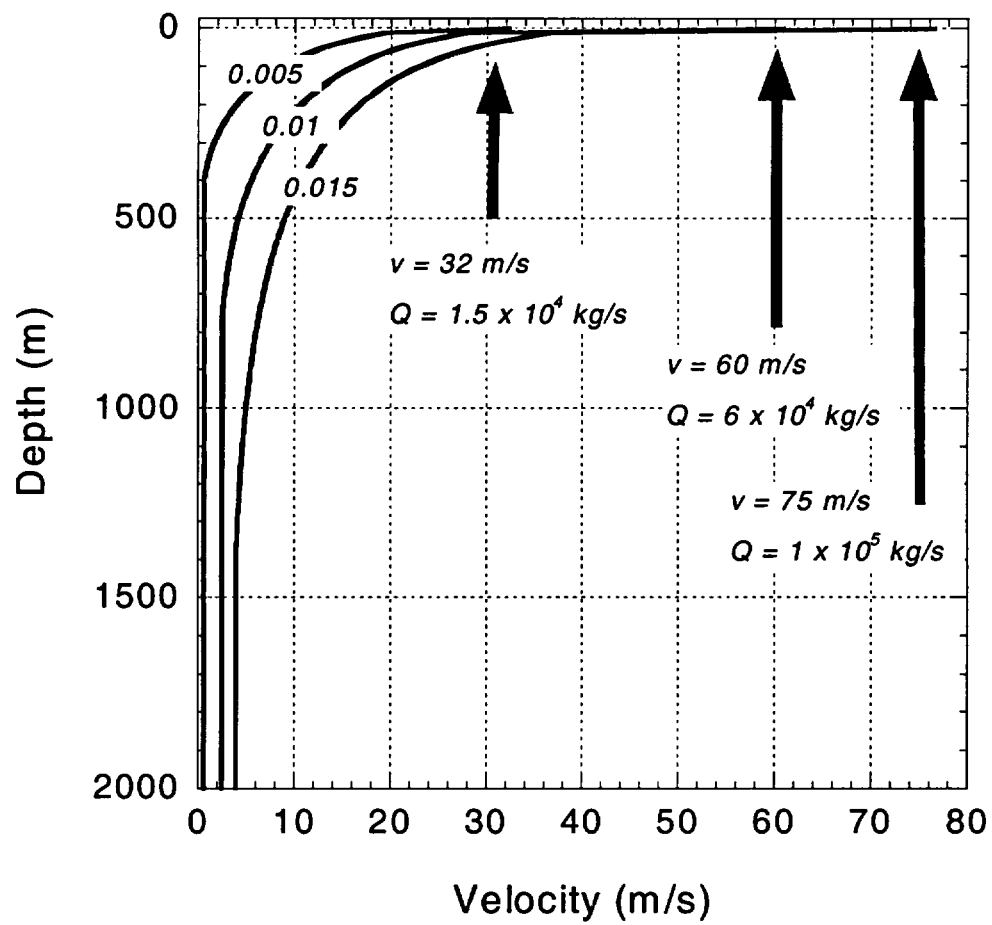


Figure 5. La Femina et al.